JOURNAL OF PROPULSION AND POWER
Vol. 16, No. 6, November–December 2000

Performance Analysis for High-Speed Missile Inlets

Christophe Bourdeau,* Michaël Blaize,* and Doyle Knight†
Rutgers University, Piscataway, New Jersey 08854-8058

A new methodology, Euler semiempirical simulation for three-dimensional inlets (2ES3D), has been developed to predict three-dimensional missile inlet aerodynamic performance within a small fraction of the time required for conventional Reynolds averaged Navier–Stokes solvers. The 2ES3D method is based on an Euler flow solver with a virtual terminal shock model and an analytical subsonic diffuser model. The details and validation of the methodology are presented.

Nomenclature

M	=	Mach number
P	=	pressure, Pa
T	=	temperature, K
ϵ	=	mass flow rate coefficient
η	=	total pressure recovery coefficient
ρ	=	density, kg/m^3

Subscripts

back	=	back pressure at the end of the diffuser
ref	=	reference values used for η and ϵ
t	=	stagnation conditions
VTS	=	virtual terminal shock

Introduction

THE aerodynamic design of high speed missile inlets is a critical problem. A large number of coupled design parameters, together with manufacturing and aerodynamic constraints, have to be addressed to achieve high performance. Consequently, automated optimization through computational software is of great interest to the aerospace industry. However, a critical barrier to automated design of high-speed inlets is the cost of evaluating the aerodynamic performance of candidate designs.

Several optimizations of intakes and nozzles have been successfully performed for two-dimensional configurations. A hypersonic inlet was optimized using a gradient-based algorithm,[1,2] and an automated optimization loop has been developed for two-dimensional supersonic missile inlets.[3,4] For the latter, both a single flight condition and a full mission optimization were considered, leading to substantial improvement of the initial performance for the whole flight domain. References 4–6 include detailed descriptions of the optimization strategy and results for two-dimensional and three-dimensional automated optimizations. However, in the case of supersonic inlets, wind-tunnel experiments as well as Reynolds averaged Navier–Stokes (RANS) simulations have proven that the flowfield inside an inlet is highly three dimensional,[7] even in the case of nominally two-dimensional geometries. Moreover, performance in side-slip conditions limits the maneuverability of the vehicles and can only be addressed through three-dimensional computations.

The performance analysis of air intakes using three-dimensional RANS methods is computationally very expensive. High-accuracy flow solvers and fine meshes are needed to simulate the complex physical phenomena occurring in the inlet duct. Consequently, these techniques cannot yet be used in an automated optimization process. This paper presents a hybrid methodology, Euler semiempirical simulation for three-dimensional inlets (2ES3D) that evaluates the inlet aerodynamic performance in three-dimensional cases, but with fewer computer resources than RANS. This methodology is based on a three-dimensional Euler flowfield computation, a model for the terminal shock system denoted the virtual terminal shock (VTS) and semiempirical corrections for the diffuser. The 2ES3D methodology has been developed to be fast and accurate enough to predict correctly trends for a wide range of three-dimensional inlet designs in an automated design optimization environment.

First, the flow solver and the hybrid methodology 2ES3D are described. Second, the VTS model is validated against Euler computations. Third, several parameters of 2ES3D are investigated, and their validity is assessed against experimental data and a validated two-dimensional inlet code (OCEAS). This study demonstrates that 2ES3D is a reliable simulation tool for a family of inlet geometries.

Flow Analysis

The function of the inlet is to provide a high-pressure, low-speed flow to the engine from the low-pressure, high-speed flowfield outside. A schematic is shown in Fig. 1. The compression must be achieved with minimal total pressure loss while capturing the required amount of flow. Drag also must be limited. In the supersonic diffuser, compression is performed through a series of oblique shocks that minimize the total pressure loss. In the throat section, downstream of the geometric throat, a terminal shock system close to a normal shock makes the transition to a subsonic flow that is further compressed in the subsonic diffuser.

The overall aerodynamic performance of the inlet is defined by two coefficients: the mass flow rate coefficient ϵ and the total pressure recovery coefficient η. The mass flow rate coefficient ϵ is the ratio of the actual mass flow going through the inlet duct to the mass flow through the capture area. The latter is the maximum amount of flow entering the inlet at freestream conditions with no angle of attack or side slip. As presented in Fig. 2, A_c is the capture area and the actual flow in the inlet goes through surface A_0. The total pressure recovery coefficient η is the ratio of the average total pressure at the end of the duct to the freestream total pressure. This coefficient reaches its maximum at the critical operating condition, when the terminal shock is located in the vicinity of the aerodynamic throat.

2ES3D

The hybrid flow solver 2ES3D comprises three parts. First, a supersonic Euler computation is performed for the entire inlet. Second, the VTS is added to account for losses in the terminal shock system. Third, a subsonic diffuser model is incorporated. The elements of the simulation loop are presented in Fig. 3. These three elements are discussed subsequently.

Viscous effects ahead of the terminal shock are ignored for two reasons. First, the strengths of shock/boundary-layer interactions

Presented as Paper 99-0611 at the AIAA 37th Aerospace Sciences Meeting, Reno, NV, 11–14 January 1999; received 11 February 1999; revision received 15 July 1999; accepted for publication 27 July 1999.

*Visiting Scientist, Department of Mechanical and Aerospace Engineering.

†Professor, Department of Mechanical and Aerospace Engineering. Associate Fellow AIAA.

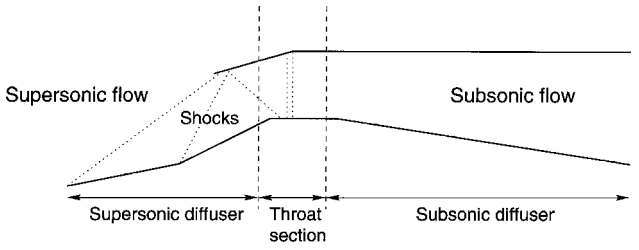

Fig. 1 Critical operating regime for a supersonic inlet.

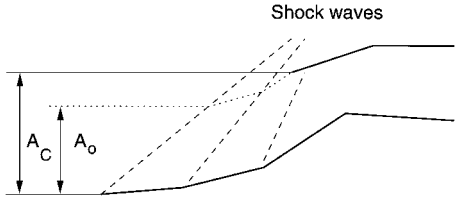

Fig. 2 Definition of mass flow rate coefficient.

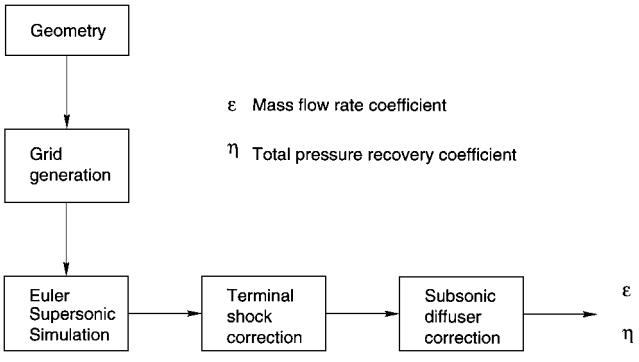

Fig. 3 Automated simulation with 2ES3D.

on the external compression ramps (Fig. 1) are typically minimized for the inlet configurations explored because the optimal external supersonic compression, that is, minimal loss in total pressure, is achieved by multiple oblique shocks (due to the ramps) of equal strength.[8] Second, the boundary layer on the compression ramps (Fig. 1) would be removed in part or entirely in an actual inlet by a boundary-layer bleed slot in the throat section. Therefore, the neglect of viscous effects ahead of the terminal shock is considered to be reasonable within the overall approximations of 2ES3D.

Supersonic Flowfield Computation

The supersonic flowfield in the inlet is simulated using GASP[9] in Euler mode. GridPro™ (Ref. 10) is used for the grid generation. A third-order upwind Van Leer scheme is used for the inviscid fluxes. A tangential boundary condition is used at the walls, and a supersonic (zero gradient) outflow boundary condition is imposed at the end of the diffuser. A single computation is performed using GASP, and the flow is supersonic from inflow to outflow except possibly for small subsonic regions that may occur under the cowl or near the geometric throat. The subsonic diffuser is modeled separately as will be described.

Missile inlets often incorporate boundary-layer bleed in the throat region after the compression ramps to minimize or eliminate boundary-layer separation that could otherwise adversely affect inlet performance. Two approaches may be taken with regard to bleed in 2ES3D. First, the bleed may be ignored in the Euler simulation, and a flow tangency boundary condition applied to all solid boundaries. Second, the bleed may be incorporated in the Euler simulation to provide a more precise estimate of the mass flow rate coefficient ϵ. The bleed plenum is not simulated but modeled using a boundary condition at the bleed inflow developed by Zha et al.[11]

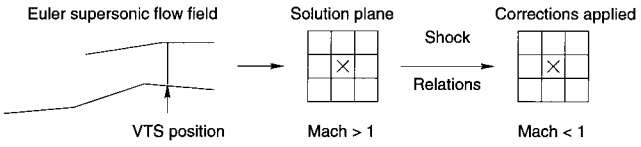

Fig. 4 VTS model.

VTS

Most of the total pressure loss in a supersonic inlet occurs within the terminal shock system. At critical operating conditions, experimental data and RANS simulations show that this shock system is positioned in the region of the boundary-layer bleed, downstream of the aerodynamic (and, typically, the geometric) throat. It is assumed that the location of the boundary-layer bleed is specified a priori. Therefore, the range of locations for the VTS is defined by the geometric throat and end of the boundary-layer bleed. At discrete points in this range, a single vertical VTS is assumed that comprises individual normal shocks within each grid cell where the flow is supersonic (Fig. 4). The Rankine–Hugoniot formulas are applied to determine the conditions downstream of the normal shock in each cell. If the flow within a cell is subsonic, the total pressure is computed directly. The average total pressure downstream of the VTS is then computed and employed as the inflow total pressure to the subsonic diffuser model.

Subsonic Diffuser

An additional total pressure loss occurs in the subsonic diffuser due to viscous effects. The boundary layer develops in an adverse pressure gradient. Some viscous effects, such as separation, can have an important effect on the inlet performance. An analytical model[12,13] is implemented to represent this behavior. The flowfield is computed using a weak–strong interaction method between the boundary layers and the nonviscous flow by means of a space-marching strategy. The core flow is one dimensional, but the boundary layers on each surface are computed. A wall function (Coles–Van Driest) is applied for the stress along the wall. The upstream conditions for the flow are the average conditions resulting from the VTS. The model takes into account the geometry of the diffuser, which is represented by various rectangular or circular cross sections. The conservation of mass and the entrainment of core flow by the boundary layer is solved. This is more accurate than simple empirical formulas, and it is able to predict the appearance and the development of separation in the diffuser with reasonable accuracy.

Description of the Generic Inlet

The test case for 2ES3D is a generic inlet that was evaluated experimentally. It is a two-dimensional inlet with boundary-layer bleed located at the geometric throat. This inlet is obtained by translating a section along an axis, which makes it two dimensional. Sidewalls connect the leading edge of the ramps to the leading edge of the cowl. Three configurations are considered, whose differences are schematically presented in Fig. 5. Configuration 1 has one compression ramp and a slanted cowl. Configuration 2 has two compression ramps and the same cowl as configuration 1. Configuration 3 has the same compression ramp as configuration 1, but its cowl is horizontal, and thus its internal compression is higher than configuration 1. Note that these inlets only vary by their compression system and have an identical bleed and subsonic diffuser.

The total pressure recovery coefficient and the mass flow rate coefficient are computed using 2ES3D for the following upstream conditions: Mach number 2.6, total pressure 1.5×10^5 Pa, total temperature 280 K, 0-deg angle of attack, and 0-deg angle of side slip.

For the experiment, only the maximum total pressure recovery coefficient and corresponding mass flow rate coefficient are available. Because there is only a single experimental data point (η, ϵ) for each configuration, all experimental data are normalized by a single reference value each for η and ϵ and are presented in Table 1. The reference values η_{ref} and ϵ_{ref} are the maximum total pressure recovery coefficient and mass flow rate coefficient from the experimental dataset. The same references are used for all of the data presented.

Table 1 Reference performance for inlets 1–3

Inlet	η/η_{ref}	$\epsilon/\epsilon_{\text{ref}}$
1	0.97	0.99
2	0.87	1.00
3	1.00	0.99

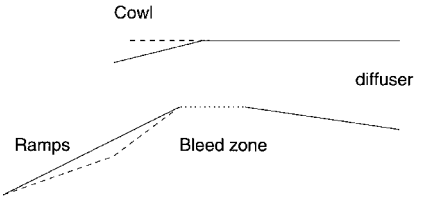

Fig. 5 Generic inlet geometry.

The experimental data defines a trend in total pressure recovery between the configurations, that is, inlet 3 is better than inlet 1, which is better than inlet 2.

The experimental inlet operating conditions were obtained by increasing the back pressure beginning with a started flow. Therefore, the experimental data are assumed to represent the critical operating condition. Although no information is available concerning the position of the normal shock system at this condition, it is expected to be in the vicinity of the throat and the bleed zone of the inlet.

Parametric Study of 2ES3D

To validate 2ES3D, several issues are addressed. First, numerical parameters for the Euler flow solver (the convergence criteria and the grid spacing) are examined. Second, the VTS model for the terminal shock is compared to an Euler computation with back pressure to evaluate the accuracy of the VTS model.

Overview

The 2ES3D method has been used to compute the flowfield for the same aerodynamic conditions as described in the preceding section. For each inlet configuration, three levels of mesh are investigated: coarse, medium, and fine. Their sizes are $46 \times 13 \times 6$ (coarse), $92 \times 26 \times 12$ (medium), and $184 \times 52 \times 24$ (fine). The geometries investigated are two dimensional, but three-dimensional meshes were actually generated to obtain estimates of CPU time for three-dimensional inlets. At the critical operating condition, the aerodynamic throat is expected to be located within the bleed zone, and therefore, various positions are investigated for the VTS model from the end of the compression ramps to the end of the bleed zone.

The calculations were performed on an SGI O2 (R5000) workstation. The CPU time needed for the Euler computation is between 5 and 10 min for the coarse mesh, 45 min and 1 h for the medium mesh, and between 10 and 16 h for the fine mesh. The CPU time is very important because 2ES3D is intended for automated design optimization. First, the flow solver convergence and grid refinement are analyzed, and second, the accuracy of the VTS model is assessed.

Convergence Analysis

To ensure that a converged flowfield is obtained from the GASP Euler solver, computations were performed using two different criteria for flowfield convergence, namely, a four order of magnitude decrease and a six order of magnitude decrease in the residual. The evaluation was performed using the coarse mesh. The convergence was evaluated for one terminal shock position with the bleed modeled. These computations using the four order and six order of magnitude decrease in the residual produced identical values ϵ and η to five significant digits. Thus, a four order of magnitude reduction in the residual is considered sufficient.

Grid Analysis

The flowfield was converged using the three different grids to assess the effect of grid refinement. The VTS model was applied at various positions in the bleed zone with bleed simulated using the Zha et al.[11] boundary condition. The results showed that the variation in mass flow rate is less than 1% between the three mesh levels. In all cases, it is slightly overevaluated, which probably results from the Euler model for the flowfield.

Figures 6–8 show the total pressure recovery coefficient vs VTS position for inlet configurations 1–3, respectively. The maximun discrepancy between the three mesh levels is less than 1% for configurations 1 and 3. The maximum discrepancy is less than 4% for configuration 2, which is higher than the other configurations due to the presence of a subsonic zone underneath the cowl.

We conclude that the coarse grid is adequate for the analysis provided the flow upstream of the VTS is entirely supersonic. The use of a coarse grid provides a substantial saving of CPU time and enables the future use of 2ES3D for a design optimization.

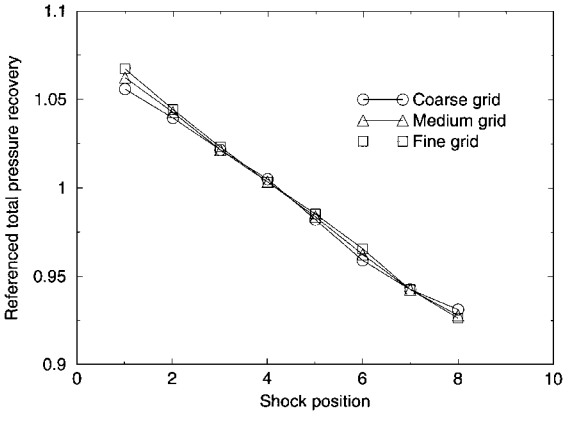

Fig. 6 Mesh influence on η/η_{ref} for inlet 1.

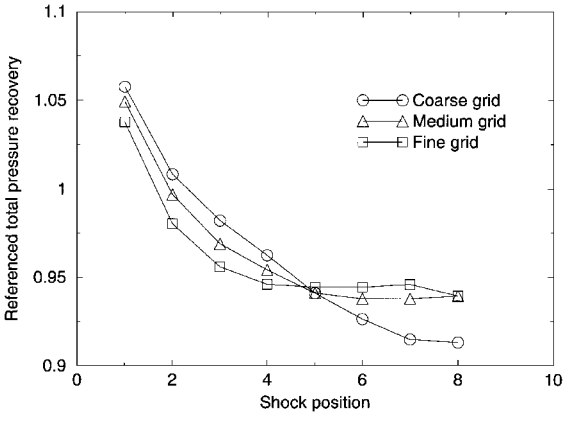

Fig. 7 Mesh influence on η/η_{ref} for inlet 2.

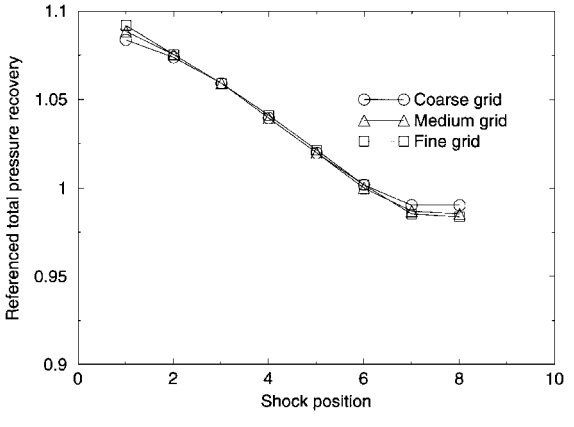

Fig. 8 Mesh influence on η/η_{ref} for inlet 3.

Validation of VTS Model

Another inlet (Fig. 9), designed using an automated optimization,[6] is used to assess the accuracy of the VTS model. This is a three ramp mixed compression inlet with lateral compression, which implies a three-dimensional flow in the duct. A three-dimensional mesh is used. The aerodynamic conditions are Mach number 3.0, total pressure 3.78×10^5 Pa, total temperature 607 K, 0-deg angle of attack and 0-deg angle of side slip. These conditions represent a typical cruise phase for a missile.

First, a completely supersonic inviscid flow is computed using GASP. Second, several computations with different back pressures are performed using the subsonic outflow boundary condition presented in the Appendix. For each back pressure, the VTS model is applied to the entirely supersonic flow using the shock position obtained from the Euler computation. Six shock locations were obtained for the terminal shock system, and their positions in the inlet duct are shown in Fig. 10.

The total pressure recovery obtained using 1) the GASP code in Euler mode and specified back pressure and 2) the GASP code in Euler model with supersonic outflow and the VTS model is presented in Table 2. The position of the VTS is known from the simulation with back pressure. In the case of shock positions 1–5, the Euler computation with back pressure shows that the normal shock has a vertical shape. The VTS in these conditions predicts the total pressure recovery within 3%. A discrepancy of 5% occurs for shock position 6, where the terminal shock shape is no longer planar but rather a curved surface from the leading edge of the cowl to the end of the third ramp. Nonetheless, even in this case, the assumed planar shape for the shock gives a good approximation for the total pressure recovery.

Table 2 VTS compared to Euler simulation with back pressure

Position	P_{back}/P_{t0}	η_{Euler}	η_{VTS}	Error, %
1	0.513	0.548	0.53	3.4
2	0.534	0.575	0.56	2.7
3	0.569	0.599	0.58	3.3
4	0.590	0.623	0.61	2.1
5	0.603	0.633	0.62	2.1
6	0.622	0.650	0.68	4.6

Fig. 9 Inlet geometry.

The position of the VTS is a variable of the VTS model. A reasonable choice could be the geometric throat; however, this position is only conditionally stable from Kantrowitz[14] theory, which shows that a normal shock is only stable in a diverging duct. Our current approach is to consider a range of locations for the VTS between the geometric throat and end of the bleed zone.

Evaluation of 2ES3D Accuracy

The accuracy of 2ES3D is evaluated by comparison with experiment and a separate inlet analysis code OCEAS (Outil de Conception d'Entre'es d'Air Supersoniques) for three configurations. In the experiment, the position of the terminal shock system at the critical operating condition is unknown, but may reliably be assumed to be downstream of the geometrical throat and in the vicinity of the boundary-layer bleed. Several VTS positions are investigated over the bleed slot for the VTS model with 2ES3D and OCEAS.

OCEAS has been developed to assist engineers in the aerodynamic design of missile inlets and has been extensively validated by comparison with experiment.[15] It is a semiempirical flow solver that uses simple and accurate physical models. This solver is limited to two-dimensional inlets with no subsonic flow upstream of the terminal shock. The supersonic flowfield is calculated by solving the Rankine–Hugoniot equations for shocks and using the Prandtl–Meyer formula for expansion fans. Boundary layers can also be modeled by their displacement effect. To find the performance for the critical operation, a terminal shock is simulated for various positions in the inlet duct. The critical operating condition is defined by the maximum total pressure recovery coefficient. Losses within the subsonic diffuser are estimated using an analytical model.[12,13] Typical CPU time is a few seconds on an SGI O2 (R5000) workstation.

In comparison with experiment, the error of OCEAS is 8% or less in total pressure recovery and 5% or less in mass capture ratio.[5] OCEAS was successfully used for the optimization of two-dimensional inlets[5] with an accurate prediction of the trend between configurations.

Analysis and Discussion

Methods 2ES3D and OCEAS give an evaluation of the mass flow rate within 3% of the experiment for all three configurations. The critical issue for the performance prediction is the total pressure recovery with loss through the shock system, and therefore, this section focuses on this point.

First, the results of the simulations performed with OCEAS are presented. Several shock positions are investigated. They define a range for η/η_{ref} as shown in Table 3. The results obtained with the three configurations bracket the experimental data. For configurations 1 and 3, the mean value is within 4% of experiment, whereas for configuration 2 the error is nearly 12%. For both configurations 1 and 3, the flow upstream of the terminal shock is entirely

Table 3 Range for η/η_{ref} with OCEAS

		OCEAS			
Inlet	Experiment	Min	Max	Mean	Error, %
1	0.97	0.968	1.049	1.009	4.0
2	0.87	0.869	1.077	0.973	11.8
3	1.00	0.969	1.059	1.014	1.4

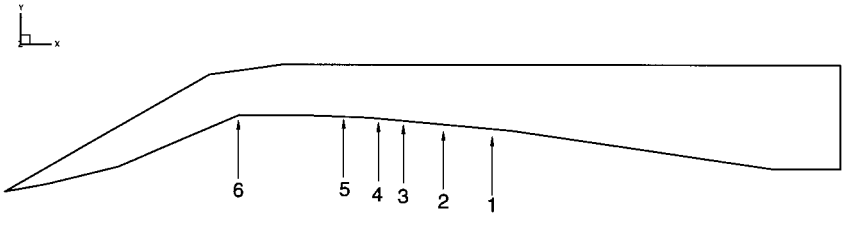

Fig. 10 Positions for the VTS.

supersonic. For configuration 2, a subsonic region exists immediately downstream of the cowl, and therefore, OCEAS is not expected to be accurate.

The total pressure recovery predicted by OCEAS for each terminal shock position is shown in Fig. 11. The trend is respected between configurations 1 and 3, that is, the total pressure recovery for configuration 3 is higher than configuration 1 as observed at the critical operating condition in the experiment (Table 1). The trend for configuration 2 is not correctly predicted for the range of terminal shock positions apparently due to the presence of a subsonic zone downstream of the cowl leading edge in the OCEAS computation.

A similar study is presented with 2ES3D in Table 4. For configurations 1 and 3, the range of values bracket the experimental data, and the mean value is within 4% of the experiment. For configuration 2, the range of values does not bracket the experiment, and the mean value is in error nearly 14%. For configuration 2, a subsonic region exists immediately upstream of the cowl, and consequently the accuracy of 2ES3D is reduced.

The total pressure recovery predicted by 2ES3D for each terminal shock position is shown in Fig. 12. The trend is respected between configurations 1 and 3 as observed for the OCEAS computations.

Figures 13–15 present a comparison of OCEAS and 2ES3D for configurations 1–3. The discrepancy between OCEAS and 2ES3D is less than 4% for configurations 1 and 3, and the behavior with shock position is similar.

In summary, 2ES3D has been shown to provide an accurate prediction of total pressure recovery and mass capture ratio provided that the flow upstream of the VTS is supersonic. The predictions of 2ES3D are insensitive to the location of the VTS within the region

Table 4 Range for η/η_{ref} with 2ES3D

		2ES3D			
Inlet	Experiment	Min	Max	Mean	Error, %
1	0.97	0.926	1.067	0.997	2.7
2	0.87	0.939	1.038	0.989	13.6
3	1.00	0.983	1.092	1.038	3.8

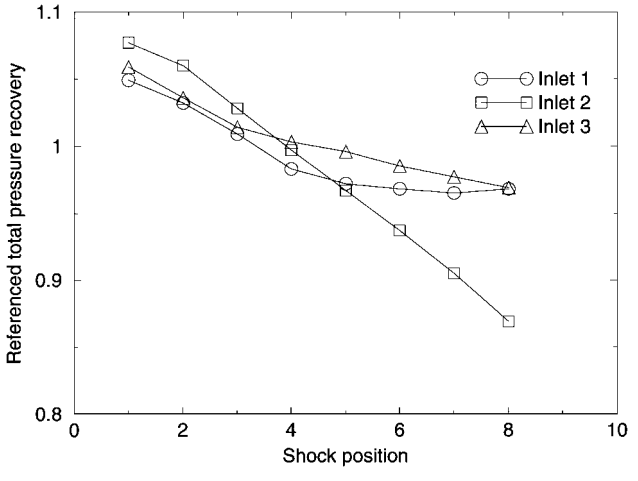

Fig. 11 Influence of the shock position on η/η_{ref} with OCEAS.

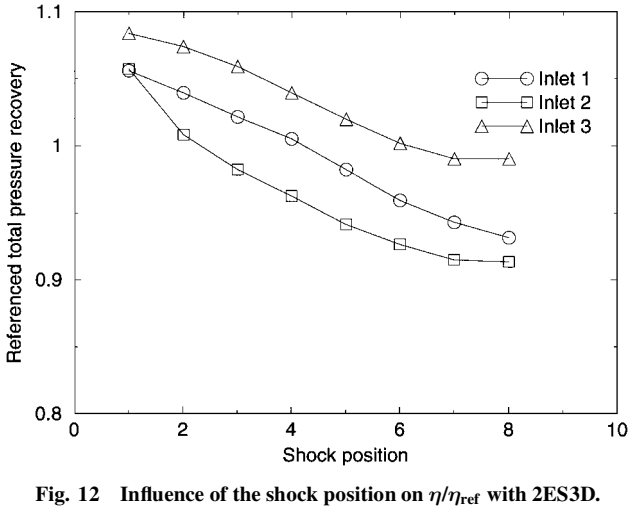

Fig. 12 Influence of the shock position on η/η_{ref} with 2ES3D.

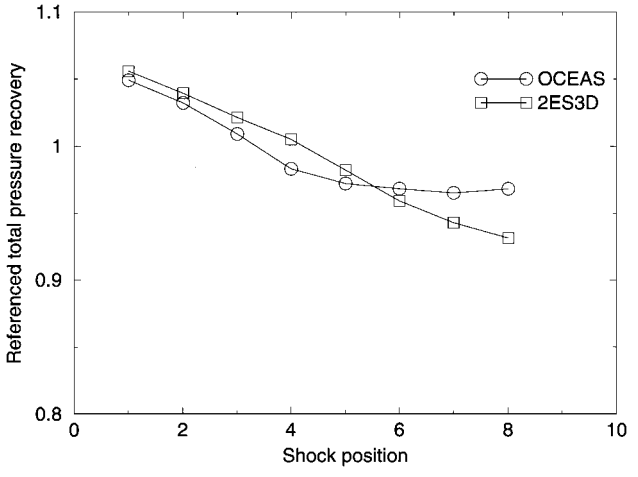

Fig. 13 Comparison between OCEAS and 2ES3D on configuration 1.

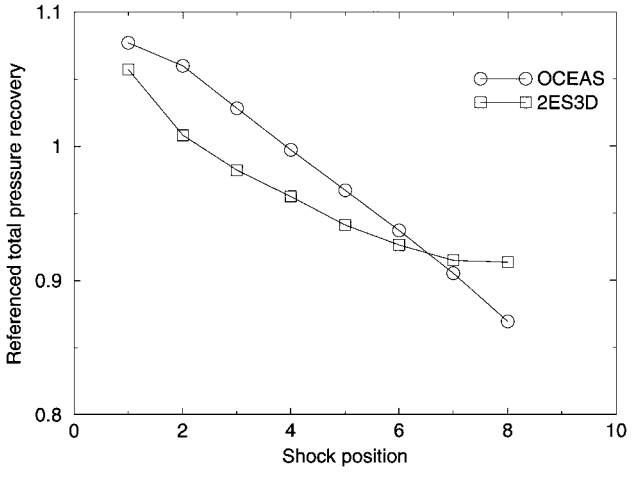

Fig. 14 Comparison between OCEAS and 2ES3D on configuration 2.

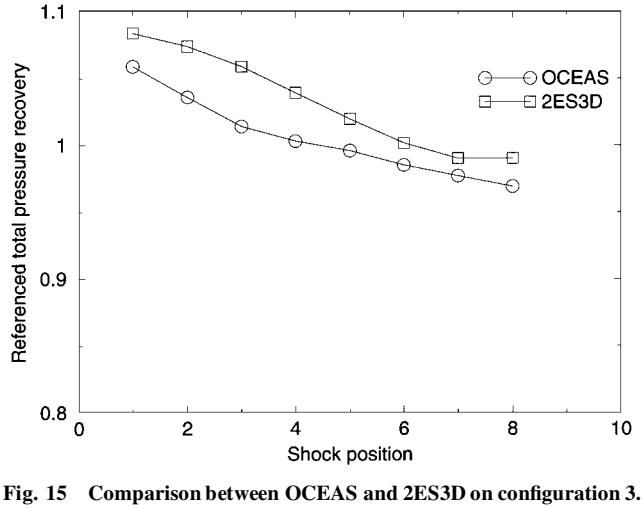

Fig. 15 Comparison between OCEAS and 2ES3D on configuration 3.

between the geometric throat and end of the boundary-layer bleed for the configurations examined. The overall accuracy of 2ES3D for these conditions is within 4% for total pressure recovery and 3% for mass capture ratio, which is comparable to OCEAS.

Conclusions

An innovative methodology 2ES3D has been developed to assess inlet performance in a reduced period of time in the perspective of automated optimization. It is based on an Euler flow solver, a VTS model, and an analytical model to compute the total pressure loss in the subsonic diffuser. The advantage of 2ES3D is its ability to analyze fully three-dimensional configurations. The VTS model is validated by comparison with Euler simulations for a three-dimensional inlet. The total pressure recovery predicted using the VTS model with a known terminal shock location is within 5% of the value obtained with a full Euler simulation with specified back pressure. The accuracy of 2ES3D is assessed by comparison with experimental data and an existing empirical code OCEAS. The experimental data comprise the total pressure recovery coefficient and mass capture ratio for three different inlets operating at the critical condition. The overall accuracy of 2ES3D for these conditions is within 4% for total pressure recovery and 3% for mass capture ratio provided the flow upstream of the VTS is entirely supersonic.

Appendix: Subsonic Outflow Boundary Condition

For the computation of an operating inlet, the influence of the engine is simulated with an imposed back pressure at the end of the diffuser. Increasing this back pressure, the terminal shock system in the diffuser moves toward an upstream position to reach the critical conditions. However, the boundary condition available in GASP for subsonic outflow (BC6) sometimes proves unable to converge the flowfield with the required decrease of the residuals to reach a steady state. This boundary condition extrapolates all variables except the pressure, which is set. A new subsonic boundary condition was developed to reach this condition. The following hypotheses are made to determine the boundary cell solution: 1) downstream pressure is set, 2) conservation of total pressure and entropy, and 3) use of theory of characteristics. As presented in Fig. A1, the inside cell solution $\boldsymbol{q}_2$ is known. From the latter and the downstream condition $\boldsymbol{q}_0$, the ghost cell solution $\boldsymbol{q}_1$ has to be evaluated. For $\boldsymbol{q}$, density ρ, speed u, v, and w, and pressure P have to be determined.

From the inside and the outside domains, the characteristics theory permits the determination of the flow speed and the speed of sound. One positive characteristic is issued from the inside domain and a negative characteristic is issued from the outside condition.[16] The flow is supposed to exit from the domain, otherwise other characteristics should be taken into account. This gives two Eqs. (A1) for u_1 and a_1 from which they can be deduced as shown in Eqs. (A2):

$$R_2^+ = u_2 + 2a_2/(\gamma - 1) = u_1 + 2a_1/(\gamma - 1)$$

$$R_0^- = u_0 - 2a_0/(\gamma - 1) = u_1 - 2a_1/(\gamma - 1) \qquad \text{(A1)}$$

$$u_1 = \left(R_2^+ + R_0^-\right)/2, \qquad a_1 = [(\gamma - 1)/4]\left(R_2^+ - R_0^-\right) \qquad \text{(A2)}$$

Equations (A2) are used to determine the velocity u_1 normal to the cell face. The other components of velocity are extrapolated from the interior, keeping the direction. To obtain density ρ_1 and pressure P_1, entropy conservation and perfect gas law are applied as

$$\rho_1 = \left(a_1^2/\gamma s_2\right)^{1/(\gamma-1)} \qquad \text{with} \qquad s_2 = P_2/\rho_2^{\gamma} \qquad \text{(A3)}$$

$$P_1 = \rho_1 a_1^2/\gamma \qquad \text{(A4)}$$

The equations for the boundary cell solution need the determination of R_2^+ and R_0^-. The former is completely defined from the solution vector $\boldsymbol{q}_2$; the latter, however, has to be expressed from the knowledge of the pressure $P_0 = P_{\text{back}}$ and the conservation of total temperature and entropy,

$$\rho_0 = \rho_2 (P_0/s_2)^{1/\gamma} \qquad \text{(A5)}$$

$$a_0 = \sqrt{\gamma P_0/\rho_0} \qquad \text{(A6)}$$

From the entropy conservation [Eq. (A5)] and given the pressure, the speed of sound a_0 for the outside condition is obtained with Eq. (A6). Then, from the total temperature T_{t0}, which is conserved during the transformation, the Mach number M_0 is obtained [Eq. (A8)], and the speed u_0 is easily deduced. With the outside flow, the boundary condition is completely defined. Thus,

$$T_0 = P_0/R\rho_0 \qquad \text{with} \qquad R = c_p - c_v \qquad \text{(A7)}$$

$$M_0 = \{[2/(\gamma - 1)](T_{t0}/T_0 - 1)\}^{\frac{1}{2}} \qquad \text{(A8)}$$

The new boundary condition cannot be imposed after a supersonic flow is converged. The entropy conservation most probably prevents any entropy drop associated with a shock. In this respect, a simulation with BC6 has to be used initially. This new boundary condition is able to converge the flowfield for positions of the shock up to the throat section in both two-dimensional and three-dimensional cases. Figure A2 shows the convergence with this boundary compared to what was obtained with BC6. An improvement appears for the convergence, and the calculated total pressure recovery is unchanged by the new condition.

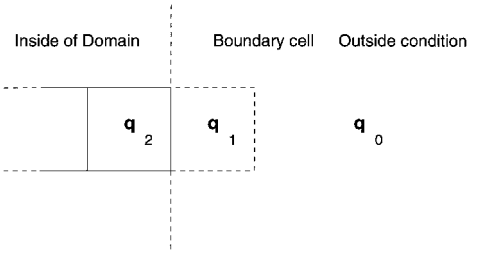

Fig. A1 Boundary cells.

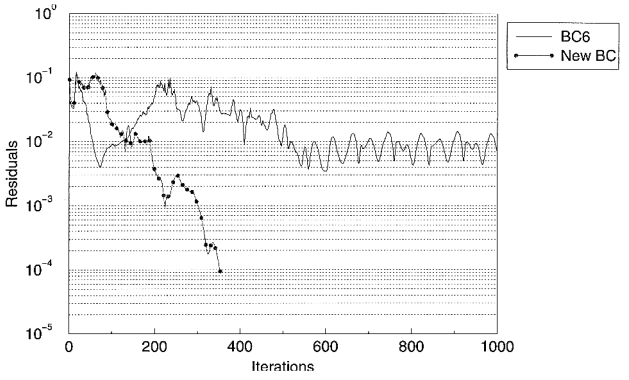

Fig. A2 Convergence for Euler calculations, P_{back} = 180 kPa.

Acknowledgments

Technical and financial support was provided by Aerospatiale Missiles and the Hypercomputing and Design Project supported by the Advanced Research Project Agency of the Department of Defense through Contract ARPA-DABT 63-93-C-0064. We would like to thank Y. Kergaravat, R. Lacau, K. Miyake, X. Montazel, K. Rasheed, and D. Smith for their invaluable assistance in this research.

References

[1]Knight, D. D., *Automated Optimal Design Using CFD and High Performance Computing*, edited by J. Palma and J. Dongarra, Lecture Notes in Computer Science, Vol. 1215, Springer-Verlag, Berlin, 1997, pp. 198–221.

[2]Shukla, V., Gelsey, A., Schwabacher, M., Smith, D., and Knight, D., "Automated Design Optimization for the P2 and P8 Hypersonic Inlets," *Journal of Aircraft*, Vol. 34, No. 2, 1997, pp. 228–235.

[3]Blaize, M., Knight, D., and Rasheed, K., "Automated Optimal Design of Two-Dimensional Supersonic Missiles Inlets," *Journal of Propulsion and Power*, Vol. 14, No. 6, 1998, pp. 890–898.

[4]Blaize, M., Knight, D., Rasheed, K., and Kergaravat, Y., "Optimal Missile Inlet Design by Means of Automated Numerical Optimization," *Proceedings of the 82nd AGARD Fluid Dynamics Panel Symposium on Missile Aerodynamics*, NATO, Research Technology Organization, Neuilly-sur-Seine, France, May 1998.

[5]Blaize, M., and Knight, D., "Automated Optimization of Two-Dimensional High Speed Missile Inlets," AIAA Paper 98-0950, Jan. 1998.

[6]Bourdeau, C., Carrier, G., Knight, D., and Rasheed, K., "Three Dimensional Optimization of Supersonic Inlets," AIAA Paper 99-2108, June 1999.

[7]Montazel, X., Kergaravat, Y., and Blaize, M., "Navier–Stokes Simulation Methodology for Supersonic Missiles Inlets," AIAA Paper 97-3147, Sept. 1997.

[8]Oswatitsch, K., "Der Druckruckgewinn bei Geschossen mit Ruckstossantrieb bei hohen Uberschallgeschwindeigkeiten (der Wirkungsgrad von Stossdiffusoren)," *Forschungen und Entwicklungen des Heereswaffenamtes, Bericht, Nr. 1005.*

[9]Applebaum, M. P., Eppard, W. M., Fury, C. B., Godfrey, A. G., McGrory, W. D., Slack, D. C., and Walters, R. W., GASP, Ver. 3, Aerosoft, Inc., 1996.

[10]Eiseman, P., GridPro™/az3000 Model 500 User's Guide and Reference Manual, Program Development Corp., White Plains, NY, 1996.

[11]Zha, G. C., Knight, D. D., Smith, D., and Haas, M., "Numerical Simulation of HSCT Inlet Operability with Angle of Attack," AIAA Paper 97-2761, July 1997.

[12]Johnston, J. P., "Diffuser Design and Performance Analysis by Unified Integral Methods," AIAA Paper 97-2733, July 1997.

[13]Childs, R. E., and Ferziger, J. H., "A Computational Method for Subsonic Compressible Flow in Diffusers," AIAA Paper 83-0505, Jan. 1983.

[14]Kantrowitz, A., "The Formation and Stability of Normal Shock Waves in Channel Flows," NACA, TR 1225, March 1947.

[15]Lacau, R. G., Garnero, P., and Gaible, F., "Computation of Supersonic Intakes," *AGARD Special Course on Missiles Aerodynamics*, AGARD Rept. 804, March 1994.

[16]Thévenin, D., "Etude et Analyse des Ecoulements Supersoniques," Ecole Centrale Paris, Paris, 1996.